

Structure of C_{60} layers on the $\text{Si}(111)-\sqrt{3}\times\sqrt{3}$ -Ag surface

Koji Tsuchie

Department of Physics, School of Science, University of Tokyo, 7-3-1 Hongo, Bunkyo-ku, Tokyo 113-0033, Japan

Tadaaki Nagao and Shuji Hasegawa*

*Department of Physics, School of Science, University of Tokyo, 7-3-1 Hongo, Bunkyo-ku, Tokyo 113-0033, Japan
and Core Research for Evolutional Science and Technology, (CREST), Japan Science and Technology Corporation (JST),
4-1-8 Honcho, Kawaguchi, Saitama 332-0012, Japan*

(Received 2 June 1999)

The structure of a monolayer of C_{60} molecules adsorbed on the $\text{Si}(111)-\sqrt{3}\times\sqrt{3}$ -Ag surface has been investigated by scanning tunneling microscopy (STM) at room temperature and at low temperature (60 K). The C_{60} molecules are arranged in a $\sqrt{21}\times\sqrt{21}(R\pm 10.9^\circ)$ double domain structure and also in a $3\sqrt{3}\times 3\sqrt{3}(R30^\circ)$ structure in part. The intramolecular structures are observed only for the molecules adsorbed at step edges at room temperature, because the rotation of C_{60} molecules is suppressed due to the strong interaction with the substrate at step edges, while the molecules adsorbed on terraces do not exhibit the internal structure because of their fast rotation. On the other hand, the internal structure of C_{60} is resolved for every molecule adsorbed on terraces at low temperature because the rotation of C_{60} is suppressed as in the C_{60} bulk crystal. The orientations of the individual C_{60} seem to be determined by the directions of underlying Si and Ag trimers of the $\sqrt{3}\times\sqrt{3}$ -Ag surface. [S0163-1829(99)03140-9]

I. INTRODUCTION

The interaction between doped or undoped C_{60} molecule layers and the underlying substrate has been investigated with various experimental techniques in recent years. In general, a C_{60} molecule is more strongly bound to metal surfaces due to large charge transfer from the substrate to C_{60} , compared with insulator surfaces such as SiO_2 and sapphire. On semiconductor surfaces, the character of the interaction strongly depends on the surface structures and the electronic states. For example, the bonding of C_{60} molecules to the

GaAs(110) surface which has a semiconducting electronic structure is van der Waals' type in character,¹ while C_{60} molecules are strongly bound to Si(111) or Si(100) clean surfaces because of the interaction with dangling bonds on the substrates, although there still remains discussion about the bonding character.²⁻⁶

Scanning tunneling microscopy (STM) is one of the most powerful tools to study the adsorption structure of C_{60} as well as the interactions between the molecules and the substrates. A lot of results of STM observations have been reported mainly on the morphology of ordered or disordered

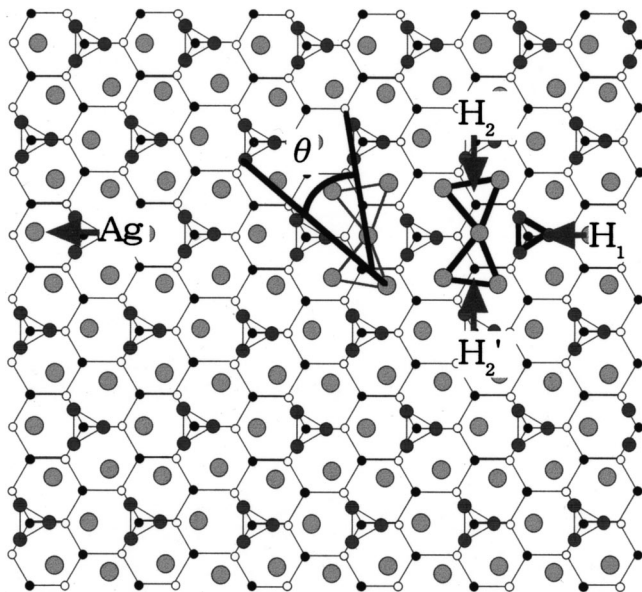


FIG. 1. Schematics of atomic arrangements for the $\text{Si}(111)-\sqrt{3}\times\sqrt{3}$ -Ag surface. The largest circles are Ag atoms, and the others are Si atoms.

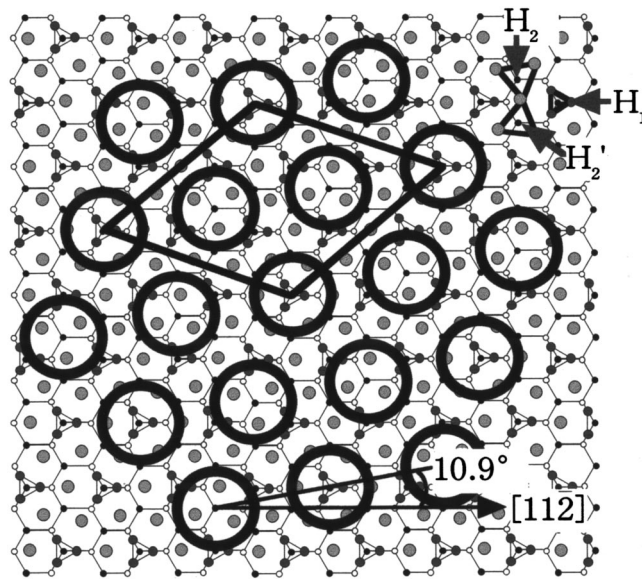


FIG. 2. An adsorption structure model for the $\text{Si}(111)-\sqrt{21}\times\sqrt{21}$ -(Ag, C_{60}) surface at RT. Large open circles represent C_{60} molecules, all of which sit at the center of Si and Ag trimers.

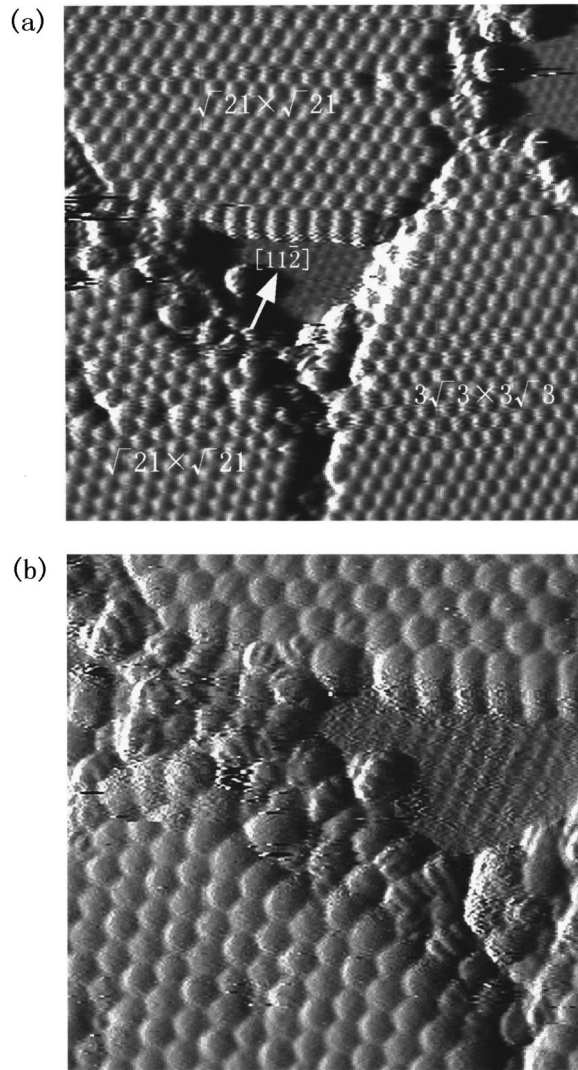


FIG. 3. (a) A $24\text{ nm} \times 24\text{ nm}$ RT-STM image of a $\text{Si}(111)\text{-}\sqrt{3} \times \sqrt{3}\text{-Ag}$ surface with a deposition of $\sim 0.8\text{ ML}$ of C_{60} at 200°C . C_{60} molecules create a $\sqrt{21} \times \sqrt{21}(R \pm 10.9^\circ)$ double domain structure and a $3\sqrt{3} \times 3\sqrt{3}(R30^\circ)$ structure. (b) A zoomed image of (a) showing an intramolecular structure of C_{60} adsorbates at a step edge (image size: $14\text{ nm} \times 14\text{ nm}$).

C_{60} islands and the intramolecular structures of individual molecules.⁷ On the $\text{Si}(111)7 \times 7$ surface, isolated C_{60} molecules are observed for a submonolayer coverage, implying that C_{60} is strongly bound to the surface and unable to migrate, although the local ordering in the C_{60} monolayer takes place at near monolayer coverage.^{8,9} Moreover, the striped internal structure is observed for isolated molecules, which means a cease of its free rotation.¹⁰ In this paper, we study the structures of C_{60} molecule layers adsorbed on the $\text{Si}(111)\text{-}\sqrt{3} \times \sqrt{3}(R30^\circ)\text{-Ag}$ surface whose atomic arrangement is resolved as HCT (honeycomb chained trimer) structure (Fig. 1).¹¹ The adsorbed Ag atoms in the HCT structure form covalent bonds with the Si atoms, leaving no dangling bonds on the surface and greatly reducing the surface reactivity. It is known that C_{60} molecules diffuse freely on the $\sqrt{3} \times \sqrt{3}\text{-Ag}$ surface and bond preferentially at defect sites and step edges, and most of the molecules form a $\sqrt{21} \times \sqrt{21}(R \pm 10.9^\circ)$ double domain structure on terraces as in

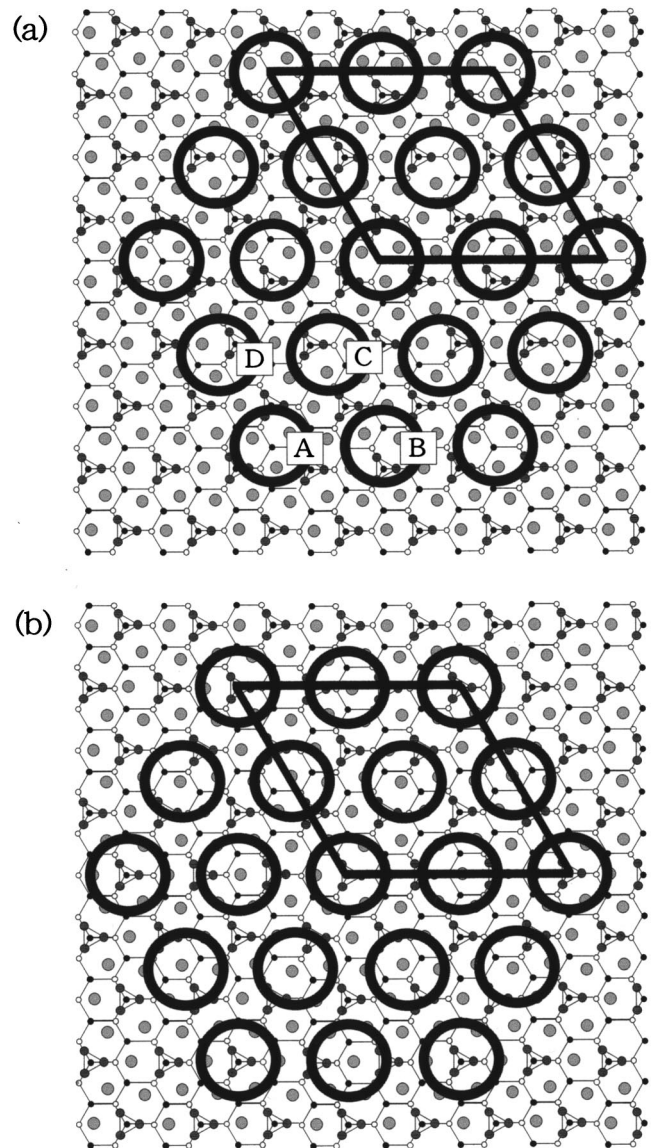
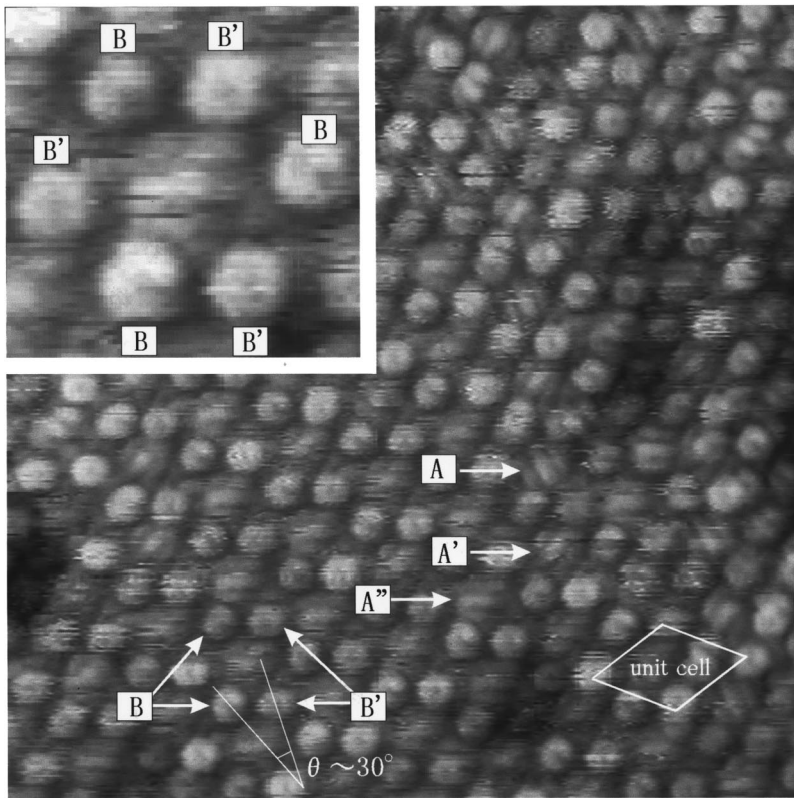


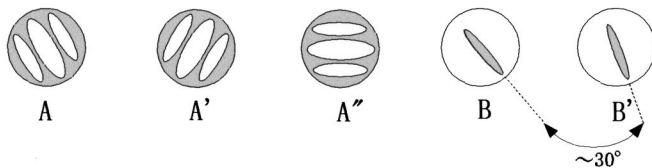
FIG. 4. Adsorption structure models for the $\text{Si}(111)\text{-}\sqrt{3} \times \sqrt{3}(R30^\circ)\text{-Ag, C}_{60}$ surface at RT, where the large open circles represent C_{60} molecules. A quarter of C_{60} molecules are located at (a) Ag trimers or (b) Si trimers, and others sit at asymmetric sites.

Fig. 2, where all of the C_{60} molecules sit above Si or Ag trimers (H_1 , H_2 , and H'_2 sites in Fig. 1).^{12,13} This system is also investigated by core-level photoemission spectroscopy, which reveals that there is no significant charge transfer from the substrate to C_{60} molecules.¹⁴

The aim of the present paper is to investigate the adsorption structure of C_{60} monolayers on the $\sqrt{3} \times \sqrt{3}\text{-Ag}$ surface by STM at room temperature (RT) and at low temperature (LT). The C_{60} molecules were found to be arranged mainly in the $\sqrt{21} \times \sqrt{21}(R \pm 10.9^\circ)$ double domain structure, and partly in a $3\sqrt{3} \times 3\sqrt{3}(R30^\circ)$ structure which was newly found in this work. These are abbreviated as $\sqrt{21} \times \sqrt{21}\text{-Ag, C}_{60}$ and $3\sqrt{3} \times 3\sqrt{3}\text{-Ag, C}_{60}$ hereafter, respectively. The molecules adsorbed at step edges presented an intramolecular structure, because the rotation of C_{60} molecules was suppressed due to the strong interaction with the substrate. On the other hand, after the sample was cooled



(a)



(b)

down to LT (60 K), the rotation of C_{60} molecules adsorbed on terraces was also suppressed as in the C_{60} bulk crystal and then the internal structures were observed for individual molecules. The internal structures depended on the adsorption sites.

II. EXPERIMENT

The experiments were performed in an ultrahigh-vacuum (UHV) system with a base pressure of 5×10^{-11} torr, equipped with a commercial STM (UNISOKU model USM501) and a reflection high-energy electron diffraction (RHEED) unit. As a substrate we used $15 \times 3 \text{ mm}^2$ pieces of a high doped p -type $\text{Si}(111)$ wafer. A clean $\text{Si}(111)-7 \times 7$ surface was obtained by flushing the sample at 1200°C several times, followed by slow cooling. The $\sqrt{3} \times \sqrt{3}$ -Ag surface was prepared by depositing 1 monolayer (ML) of Ag at a rate of 0.1 ML/min onto the 7×7 surface kept at 500°C . C_{60} molecules (more than 99.9% in purity) were sublimed onto the $\sqrt{3} \times \sqrt{3}$ -Ag surface at a rate of ~ 0.1 ML/min from a Knudsen cell held at 400°C . The substrate was held at $\sim 200^\circ\text{C}$ during the deposition, which led to the formation of large and well-ordered two-dimensional (2D) islands of C_{60} . Potassium depositions on the C_{60} molecule layer were done using a SAES dispenser installed at about 15 cm away from

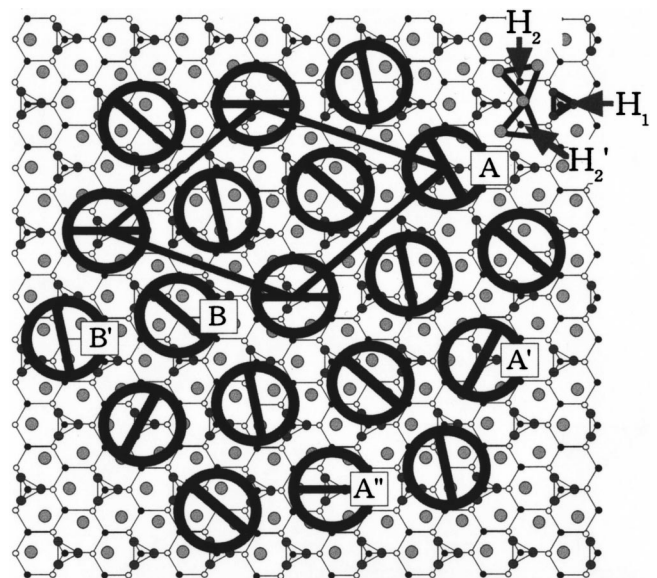


FIG. 6. An adsorption structure model for the $\text{Si}(111)-\sqrt{21} \times \sqrt{21}(R \pm 10.9^\circ)$ - (Ag, C_{60}) surface at LT, where the lines in large circles (C_{60} molecules) represent their orientations, and A (A' , A''), B, and B' correspond to those in Fig. 5.

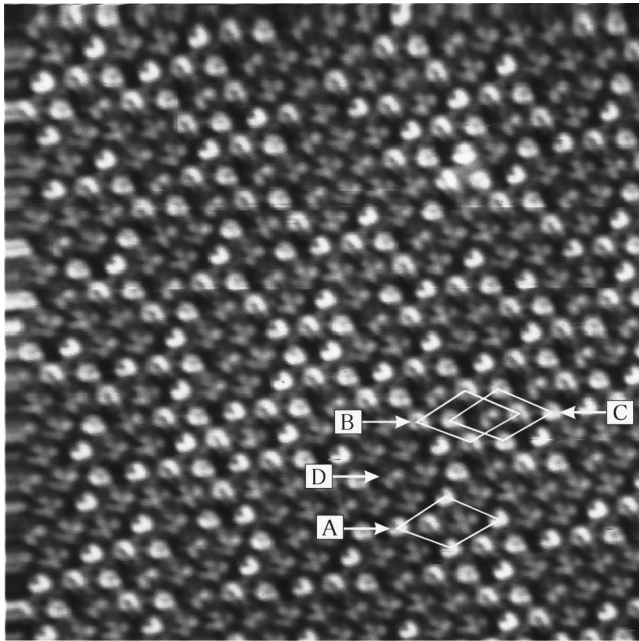


FIG. 7. A $19\text{ nm} \times 19\text{ nm}$ STM image at 60 K taken from a $\text{Si}(111)-\sqrt{21} \times \sqrt{21}(R \pm 10.9^\circ)$ - $(\text{Ag}, \text{C}_{60}, \text{K})$ surface with K doping at RT. C_{60} molecules labeled as A, B, and C have a U-like shape and those labeled as D have a three-lobe shape.

the sample. A sharp $\sqrt{21} \times \sqrt{21}(R \pm 10.9^\circ)$ RHEED pattern was produced by depositing ~ 1 ML of C_{60} onto the $\sqrt{3} \times \sqrt{3}$ -Ag surface. Note that 1 ML of C_{60} was defined as the molecule density for which the available surface area was completely covered with a close-packed hard-sphere layer

with the intermolecular spacing in bulk C_{60} , 1.005 nm. After these preparations, the sample was transferred to the STM stage, which could be cooled down to 60 K by evacuating a liquid N_2 vessel. Electrochemically etched polycrystalline W tips were used for STM imaging. The tips were cleaned in UHV by electron bombardment. The STM images shown here were taken in topographic (constant current) mode or in current-imaging mode (constant height mode only with slow feedback) with a tip bias of +2.0 V and a tunneling current of 0.4 nA (filled state imaging).

III. RESULTS AND DISCUSSION

A. RT observation

Figure 3(a) shows a STM image at RT in the current imaging mode, prepared by depositing ~ 0.8 ML of C_{60} at 200°C . Uncovered areas showing the $\sqrt{3} \times \sqrt{3}$ -Ag structure of the substrate are seen in the upper right and the center parts of the image. The upper and lower left parts of the image show the $\sqrt{21} \times \sqrt{21}(R \pm 10.9^\circ)$ - $(\text{Ag}, \text{C}_{60})$ double domains whose principal axes deviate $\pm 10.9^\circ$ from $[11\bar{2}]$ direction. In addition, another domain whose principal axis is oriented in $[11\bar{2}]$ is seen in the lower right part. The intermolecular spacing in this domain is estimated to be 1.00 ± 0.01 nm, compared with 1.016 nm in the $\sqrt{21} \times \sqrt{21}$ - $(\text{Ag}, \text{C}_{60})$ domain. Then, the periodicity in this domain is assigned to be $3\sqrt{3} \times 3\sqrt{3}(R30^\circ)$, for which two kinds of adsorption structure models are depicted in Fig. 4, where the large open circles represent C_{60} molecules. A quarter of C_{60} molecules are located at the center of (a) Ag trimers or (b) Si trimers with a period of $3\sqrt{3} \times 3\sqrt{3}$ and other

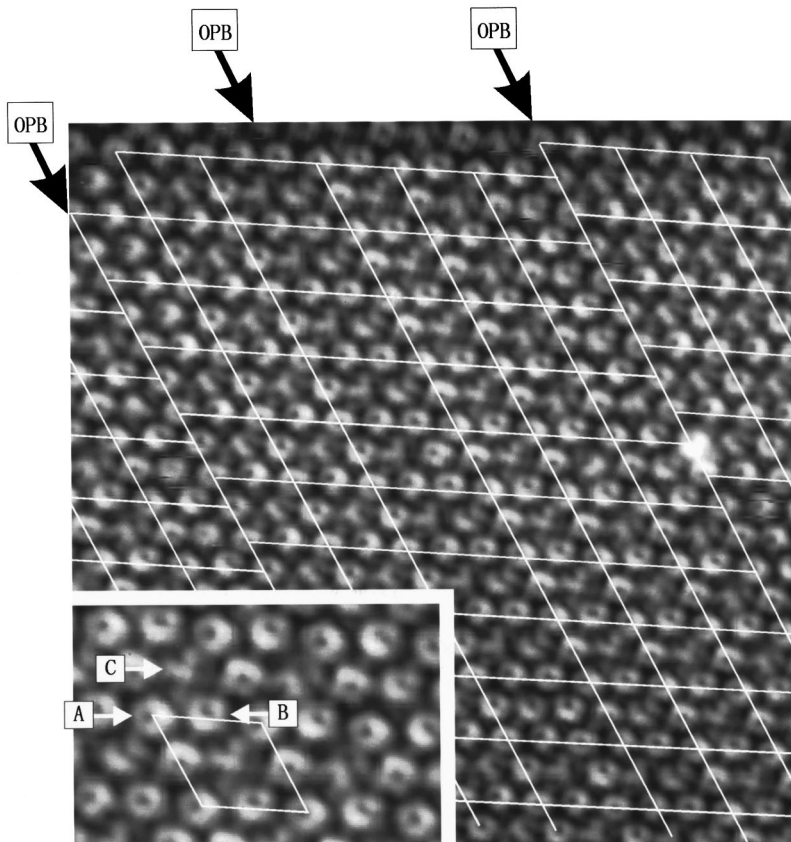


FIG. 8. (a) A $19\text{ nm} \times 19\text{ nm}$ STM image of a $\text{Si}(111)-3\sqrt{3} \times 3\sqrt{3}(R30^\circ)$ - $(\text{Ag}, \text{C}_{60}, \text{K})$ surface at 60 K. Two different kinds of molecules, i.e., those in U-like shape (shown by A and B) and those in three-lobe shape (shown by C), are observed, forming a $3\sqrt{3} \times 3\sqrt{3}$ unit cell illustrated in the inset. One can see out-of-phase domain boundaries (OPB) shown by arrows.

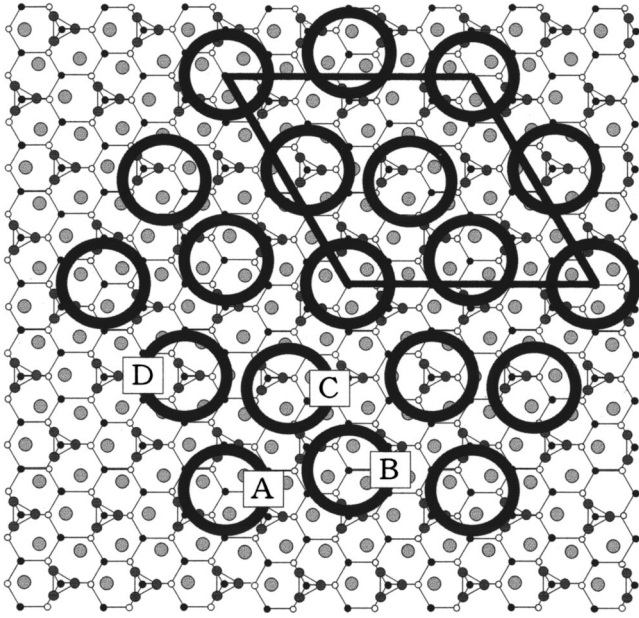


FIG. 9. An adsorption structure model for the $Si(111)-3\sqrt{3}\times 3\sqrt{3}(R30^\circ)-(Ag, C_{60}, K)$ surface at LT, which is made by moving some molecules at asymmetric sites (B and D in Fig. 4) toward the center of Ag or Si trimers nearby. So three-quarters of C_{60} molecules sit at the center of Si and Ag trimers, while only a quarter of them (indicated by C) are still located at asymmetric sites.

sit at asymmetric sites. The intermolecular spacing in this arrangement is $\frac{3}{2}\sqrt{3}a_0=0.998$ nm, where a_0 is the lattice constant of $Si(111)$ surface.

As far as we observed, there were no isolated molecules and few domain boundaries on defect-free terraces. This indicates that the interaction between the adsorbates and the substrate is so weak that the diffusion length of C_{60} at 200 °C is much longer than the terrace width (typically ~ 0.1 μm). Then we can assume that the interaction potential for a pair of C_{60} on the surface is approximated by that for free C_{60} molecules¹⁵ calculated by Girifalco.¹⁶ The Girifalco potential reveals that the interaction energy is almost the same for the $\sqrt{21}\times\sqrt{21}$ and the $3\sqrt{3}\times 3\sqrt{3}$ structures because the intermolecular distances are quite similar in both structures. Nevertheless, the ratio of the total area of the $3\sqrt{3}\times 3\sqrt{3}$ domain to that of the $\sqrt{21}\times\sqrt{21}$ domain was very small, for the RHEED spots associated with the $3\sqrt{3}\times 3\sqrt{3}$ structure were hardly observed, although the typical size of each domain was not so different in the STM image. The $\sqrt{21}\times\sqrt{21}$ domain may be energetically favorable, because, as Upward *et al.* argued,¹² all of the C_{60} molecules sit at stable sites of the center of Ag or Si trimers (see Fig. 2), while only a quarter of C_{60} molecules occupy such sites in the $3\sqrt{3}\times 3\sqrt{3}$ structure (see Fig. 4).

In Fig. 3(b), which is a close examination of the center part of Fig. 3(a), we can see striped intramolecular structures of C_{60} molecules adsorbed at a step edge running from the upper left to the lower right corners. It is known that C_{60} molecules are rotating in their bulk crystals at a rate of 10^9 s^{-1} at RT.¹⁷ The fact that the intramolecular structure of the molecules is observed only at step edges means that the rotation of the molecules is suppressed due to the strong bonding only at step edges, while the C_{60} molecules ad-

sorbed on terraces are still free to rotate as in the C_{60} bulk crystal because of the weak interaction with the substrate. The similar striped structures in individual molecules are also observed in other systems.¹⁰

B. LT observations

Figure 5(a) shows an STM topographic image obtained from the $\sqrt{21}\times\sqrt{21}-(Ag, C_{60})$ surface at 60 K. We can expect that the rotation of C_{60} molecules on terraces is suppressed at LT as in the C_{60} bulk crystal.^{18,19} Indeed, the intramolecular structures of individual molecules are seen in the image. The structures are roughly divided into two types, that is, a striped structure [shown by A , A' , and A'' in Fig. 5(a)] and a \odot -shaped structure (shown by B and B') which are schematically illustrated in Fig. 5(b). Each of A , B , and B' is arranged with a period of $\sqrt{21}\times\sqrt{21}$, shown with a unit cell at the lower right corner. Furthermore, the directions of the stripes in A , A' , and A'' types rotate by 120° with one another, and B and B' types make an angle of approximately 30° . Together with the fact that the electronic states at H_2 and H_2' sites in Fig. 1 are almost the same and different from H_1 sites, the C_{60} molecules of A (and A' , A'') and B (and B') types can be considered to be located at H_1 and H_2 (and H_2') sites, respectively. Then the difference of the orientation among A , A' , and A'' is attributed to the threefold symmetry of the underlying Si trimers at H_1 sites, and the angle between the stripes of B and B' is attributed to two kinds of Ag trimers at H_2 and H_2' sites under them (shown by θ in Fig. 1). We therefore argue that the free rotation of C_{60} molecules on the $\sqrt{3}\times\sqrt{3}$ -Ag surface is suppressed at LT and their orientations are determined by the directions of the underlying Si and Ag trimers of the substrate. This is qualitatively different from the case of Fig. 3 at RT, in which the rotation of C_{60} is suppressed only at step edges due to the strong bonding to the substrate.

Figure 6 shows an adsorption structure model for the $\sqrt{21}\times\sqrt{21}-(Ag, C_{60})$ surface at LT, where the lines in large circles (C_{60} molecules) represent their orientations and A (A' , A''), B , and B' correspond to those in Fig. 5.

C. With K doping

The $\sqrt{21}\times\sqrt{21}$ RHEED pattern became clearer after the deposition of a moderate quantity of K. It was likely that K atoms were incorporated into the interstitial sites in the $\sqrt{21}\times\sqrt{21}$ domains, and the electron beam was scattered by those atoms whose atomic scattering factor was much larger than that of C atoms. Figure 7 shows an STM topographic image at 60 K obtained from the $\sqrt{21}\times\sqrt{21}-(Ag, C_{60})$ structure after additional deposition of K at RT. We can see two kinds of molecules: U-like shaped ones (marked by A , B , and C) and three-lobe-shaped ones (marked by D). The orientations of A , B , and C are different and each of the molecules is arranged with a period of $\sqrt{21}\times\sqrt{21}$ (lozenges indicate their unit cells). Their orientations seem to be determined by the directions of the underlying Si and Ag trimers on the substrate, while the orientation of the lobes in the D -type molecules is not correlated with the substrate. In this way, by doping K into the $\sqrt{21}\times\sqrt{21}-(Ag, C_{60})$ layer, its electric structure and the resulting STM image seem to

change from the undoped $\sqrt{21} \times \sqrt{21}$ -(Ag, C_{60}) phase shown in Fig. 5. A clear difference between the U-like shaped and three-lobe-shaped molecules in the image, which is not seen in the undoped C_{60} layer in Fig. 5, may come from inhomogeneity in electron transfer from K atoms.

Apparently different were the STM images of the $3\sqrt{3} \times 3\sqrt{3}$ -(Ag, C_{60}) surface between RT and LT, although little change was introduced by K-atom incorporation in this phase. Figure 8 shows a STM topographic image obtained from the $3\sqrt{3} \times 3\sqrt{3}$ -($\text{Ag}, \text{C}_{60}, \text{K}$) surface at 60 K. Two different kinds of molecules, i.e., U-like shaped ones (shown by *A* and *B*) and three-lobe-shaped ones (shown by *C*) were observed as in the $\sqrt{21} \times \sqrt{21}$ -($\text{Ag}, \text{C}_{60}, \text{K}$) in Fig. 7. *A* and *B* are oriented in different directions, forming a $3\sqrt{3} \times 3\sqrt{3}$ unit cell illustrated in the inset; the center of the unit cell is occupied by a molecule of type *C*. We can see out-of-phase domain boundaries (OPB) in Fig. 8, where the unit mesh of the $3\sqrt{3} \times 3\sqrt{3}$ structure is superimposed.

We can make a model of the $3\sqrt{3} \times 3\sqrt{3}$ structure by moving some molecules sitting at asymmetric sites in Fig. 4 (indicated by *B* and *D*) toward the centers of Ag or Si trimers nearby, which is depicted in Fig. 9. In this arrangement, only the molecule *C* at the center of the unit cell, showing a three-lobe shape in Fig. 8, is located at an asymmetric site, while the molecules *A*, *B*, and *D* showing a U-like shape in Fig. 8 sit at the center of Ag or Si trimers. The distance between *B* (or *D*) and *C*, however, is so small (~ 0.8 nm) that a large repulsive force may act between them. The molecule *C* at the asymmetric site may slightly move outwards in the direction normal to the surface to avoid the repulsive force and to decrease the total free energy of the surface.

IV. SUMMARY

We have investigated the adsorption structures and the intramolecular structures of monomolecular layers of C_{60} deposited on the $\text{Si}(111)\text{-}\sqrt{3} \times \sqrt{3}(R30^\circ)\text{-Ag}$ surface by STM and RHEED. The C_{60} layers present $\sqrt{21} \times \sqrt{21}(R \pm 10.9^\circ)$

double domains and also $3\sqrt{3} \times 3\sqrt{3}(R30^\circ)$ domains. The former is a stabler structure because all C_{60} molecules in the $\sqrt{21} \times \sqrt{21}$ domains are located at the centers of Si and Ag trimers, which are stable adsorption sites, while some molecules in the $3\sqrt{3} \times 3\sqrt{3}$ domains sit at asymmetric sites on the substrate.

The striped structures are observed in the individual molecules adsorbed at step edges at RT, because the rotation of C_{60} molecules is suppressed due to the strong interaction with the substrate only at step edges. However, the internal structures of C_{60} are resolved even for individual molecules adsorbed on terraces at LT. The rotation of C_{60} is suppressed at LT also on terraces and the molecule orientations seem to be determined by the directions of the underlying Si and Ag trimers on the substrate.

According to our valence-band photoemission spectroscopy²⁰ and core-level one,¹⁴ the interaction between C_{60} molecules and the $\sqrt{3} \times \sqrt{3}\text{-Ag}$ surface is quite weak. However, a very small amount of charge transfer between them seems to occur as suggested by electron-energy-loss spectroscopy.²¹ Such a weak interaction with the substrate, but not a pure van der Waals type, causes the superstructures such as $\sqrt{21} \times \sqrt{21}$ and $3\sqrt{3} \times 3\sqrt{3}$, though intermolecular interactions may also play a role in the phenomena observed here.

ACKNOWLEDGMENTS

This work has been supported in part by Grants-in-Aid for Scientific Research from the Ministry of Education, Science, Culture, and Sports of Japan, especially through the Grant-in-Aid for Creative Basic Scientific Research (No. 09NP1201) conducted by Professor K. Yagi of Tokyo Institute of Technology. We have been supported also by CREST (Core Research for Evolutional Science and Technology) of the Japan Science and Technology Corporation (JST) conducted by Professor M. Aono of Osaka University and RIKEN.

*Electronic address: shuji@surface.phys.s.u-tokyo.ac.jp

¹Y. Z. Li, M. Chander, J. C. Partin, J. H. Weaver, L. P. F. Chibante, and R. E. Smalley, *Science* **253**, 429 (1991).

²S. Suto, K. Sakamoto, T. Wakita, C. Hu, and A. Kasuya, *Phys. Rev. B* **56**, 7439 (1997).

³Y. Fujikawa, K. Saiki, and A. Koma, *Phys. Rev. B* **56**, 12 124 (1997).

⁴P. Moriarty, M. D. Upward, A. W. Dunn, Y.-R. Ma, and P. H. Béton, *Phys. Rev. B* **57**, 362 (1998).

⁵T. Pi, L. Hong, R. Wu, C. Cheng, and M. Ko, *Surf. Rev. Lett.* **5**, 101 (1998).

⁶K. Sakamoto, M. Harada, D. Kondo, A. Kimura, A. Kakizaki, and S. Suto, *Phys. Rev. B* **58**, 13951 (1998).

⁷T. Sakurai, X.-D. Wang, Q. K. Xue, Y. Hasegawa, T. Hashizume, and H. Shinohara, *Prog. Surf. Sci.* **51**, 263 (1996).

⁸T. Sato, T. Sueyoshi, and M. Iwatsuki, *Surf. Sci.* **321**, L137 (1994).

⁹D. Chen, J. Chen, and D. Sarid, *Phys. Rev. B* **50**, 10 905 (1994).

¹⁰T. Hashizume and T. Sakurai, *Sci. Rep. Res. Inst. Tohoku Univ.* **A 44**, 17 (1997).

¹¹T. Takahashi and S. Nakatani, *Surf. Sci.* **282**, 17 (1993).

¹²M. D. Upward, P. Moriarty, and P. H. Béton, *Phys. Rev. B* **56**, R1704 (1997).

¹³T. Nakayama, J. Onoe, K. Takeuchi, and M. Aono, *Phys. Rev. B* **59**, 12 627 (1999).

¹⁴G. Le Lay, M. Gothelid, V. Yu. Aristov, A. Cricenti, M. C. Hakansson, C. Giammichele, P. Perfetti, J. Avila, and M. C. Asensio, *Surf. Sci.* **377-379**, 1061 (1997).

¹⁵Ch. Girard, Ph. Lambin, A. Dereux, and A. A. Lucas, *Phys. Rev. B* **49**, 11 425 (1994).

¹⁶L. A. Girifalco, *J. Phys. Chem.* **96**, 858 (1992).

¹⁷O. Zhou, J. E. Fischer, N. Coustel, S. Kycia, Q. Zhu, A. R. McGhie, W. J. Romanow, J. P. McCauley, A. B. Smith, and D. E. Cox, *Nature (London)* **351**, 462 (1991).

¹⁸P. A. Heiney, J. E. Fisher, A. R. McGhie, W. J. Romanow, A. M. Denenstien, J. P. McCauley Jr., A. B. Smith III, and D. E. Cox, *Phys. Rev. Lett.* **66**, 2911 (1991).

¹⁹W. I. F. David, R. M. Ibberson, T. J. S. Dennis, J. P. Hare, and K. Praasides, *Europhys. Lett.* **18**, 219 (1992).

²⁰K. Tsuchie, I. Matsuda, S. Oouchi, T. Tanikawa, K. Horikoshi, H. W. Yeom, and S. Hasegawa (unpublished).

²¹K. Iizumi, K. Ueno, K. Saiki, and A. Koma (unpublished).